Evaluation and improvement of end-to-end bandwidth measurement method for power-saving routers

Daisuke Kobayashi*, Go Hasegawa†, Masayuki Murata*
*Graduate School of Information Science and Technology, Osaka University
1-5 Yamadaoka, Suita, Osaka, Japan
Email: {d-kobays, murata}@ist.osaka-u.ac.jp
†Cybermedia Center, Osaka University
1-32 Machikaneyama, Toyonaka, Osaka, Japan
Email: hasegawa@cmc.osaka-u.ac.jp

Abstract—The increase in energy consumption associated with ever-intensifying network traffic is becoming a major problem. A number of researchers have focused on technologies that dynamically adjust the processing performance and the link speed of routers according to the network traffic load in order to achieve energy-efficient networking. However, when such power-saving routers are present in an end-to-end network path, the accuracy of existing methods for measuring the end-to-end available bandwidth may degrade because of the variable bandwidth and delays at bottleneck links. Furthermore, the energy efficiency of power-saving routers also decreases under the additional traffic load caused by bandwidth probing. In this paper, we employ a network environment with a power-saving router to evaluate the performance of Pathload, which is a popular tool for measuring the end-to-end available bandwidth. By showing detailed simulation results, we demonstrate that both the measurement accuracy of Pathload and the energy efficiency of routers degrade, particularly when the power saving function of routers is triggered in shorter cycles. We also propose Pathload parameter settings that maintain measurement accuracy without affecting the behavior of power-saving routers.

Keywords-available bandwidth; bandwidth measurement; energy efficiency; router;

I. INTRODUCTION

The increase in energy consumption in computer networks associated with the constant intensification of network traffic is becoming a major problem. Many researchers are studying methods for energy-efficient networking by introducing power-saving routers and switches which adjust their processing performance and link speed according to the network traffic load. For example, a power saving method for Gigabit Passive Optical Network (G-PON) was introduced [1] in which routers adjust their link speed to either 1 Gbps or 10 Gbps and enter sleep mode according to the network traffic load. Power saving techniques for Ethernet adapters with adaptive link rates [2], ADSL2 and ADSL2+ [3] have also been proposed.

However, the effect of such power-saving routers and switches on end-to-end network controls and protocols has not been investigated in detail. In this regard, we focus on an end-to-end bandwidth measurement method. When power-saving routers and switches are present in an end-to-end network path, the round trip time (RTT) of the path varies since packet processing delays at such links fluctuate. As a result, the accuracy of existing measurement methods for end-to-end available bandwidth may degrade, while end-to-end bandwidth measurement is becoming increasingly important for such network environments with variable physical capacity.

Numerous tools for measuring end-to-end available bandwidth have been developed, such as Pathload [4], ImTCP [5] and others [6-11]. However, these tools do not take into account environments where the physical link bandwidth changes according to the network load. Furthermore, since most measurement methods involve sending probing packets at an extremely high rate, the energy efficiency of power-saving routers may degrade under the additional traffic load caused by bandwidth probing.

In this paper, as a first step toward tackling the above problems, we employ an environment with a power-saving router and evaluate the performance of Pathload, which is a popular tool for measuring end-to-end available bandwidth and its measurement principle is applied in many other bandwidth measurement tools. We explore the interaction between the bandwidth measurement tool and the power-saving router. In addition, we conduct a simple mathematical analysis on the impact of bandwidth measurement using Pathload on power-saving routers and propose Pathload parameter settings that maintain measurement accuracy without affecting the behavior of power-saving routers.

The rest of this paper is organized as follows. Section II provides an overview of power-saving routers and the algorithm that they employ for adjusting the bandwidth according to network traffic load. In Section III, we evaluate the performance of Pathload in a network environment with power-saving routers by simulation experiments and reveal the problems to be solved. Section VI provides guidelines in terms of parameter settings for Pathload based on mathematical analysis. Finally, we conclude this paper and present

goals for future work in Section V.

II. POWER-SAVING ROUTER MODEL

In this section, we present a model of a power-saving router that regulates its physical link bandwidth according to the network traffic load. We construct the model based on the proposal by Ata et al., who described the conceptual design and the details of various implementation issues associated with power-saving routers [12].

We assume that the power-saving router monitors its link utilization at regular intervals (of the order of milliseconds to seconds) and regulates its physical bandwidth according to the observed utilization. We define the maximum value of the physical link bandwidth, in other words, the link bandwidth without power saving, as C_{max}. Assuming an N-level stepwise power saving configuration, the i th setting of the physical bandwidth, denoted as C_i, is defined as follows.

$$C_i = \frac{i}{N} C_{max} (1 \leq i \leq N) \qquad (1)$$

We define τ as the length of the interval for monitoring link utilization and assume that the power-saving router changes the link bandwidth at the same cycle. $P(t)$ and $C(t)$ represent the amount of traffic observed at the link and the physical link bandwidth at t th time slot, respectively. In this case, the link utilization $u(t)$ is represented as follows.

$$u(t) = \frac{P(t)}{C(t)\tau} \qquad (2)$$

The average link utilization $U(t)$ at the t th time slot is expressed as an exponential moving average.

$$U(t) = (1-w)U(t-1) + wu(t) \qquad (3)$$

The parameter w in Eq. (3) is the averaging weight. The power-saving router determines the physical link bandwidth at the $(t+1)$th time slot according to the following equations.

$$C(t+1) = \begin{cases} C_{i+1} & \text{if } U(t) \geq \lambda_u \text{ and } i < N \\ C_{i-1} & \text{if } U(t) \leq \lambda_l \text{ and } i > 1 \\ C_i & \text{otherwise} \end{cases} \qquad (4)$$

The parameters λ_u and λ_l in Eq. (4) are thresholds of the link utilization which are used to determine whether the power-saving router should increase or decrease its physical link bandwidth, respectively. From Eq. (4), it follows that the power-saving router increases its physical link bandwidth when the average link utilization becomes larger than λ_u and decreases the bandwidth when the average link utilization becomes smaller than λ_l.

III. EVALUATION OF PATHLOAD WITH A POWER-SAVING ROUTER

We evaluate the performance of Pathload in an environment with power-saving routers whose behaviors are defined
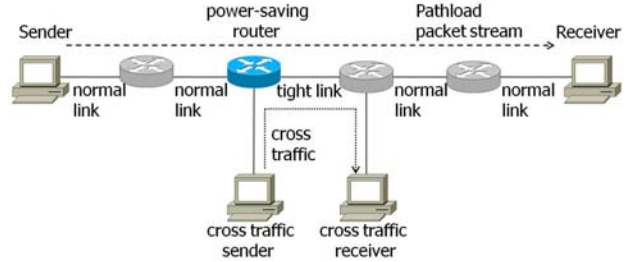
Figure 1. Network topology for simulation experiments

Table I
PARAMETERS OF THE POWER-SAVING ROUTER

Parameter	Variable	Value
Maximum value of physical link bandwidth	C_{max}	2000 Mbps, 1000 Mbps, 100 Mbps
Number of steps for regulating physical bandwidth	N	10
Upper threshold of link utilization for increasing physical bandwidth	λ_u	0.8
Lower threshold of link utilization for decreasing physical bandwidth	λ_l	0.3
Averaging weight	w	0.3
Length of the interval for monitoring link utilization	τ	100, 10, 5, 1 ms

in the previous section, by conducting simulation experiments with the ns-2 network simulator [13]. We evaluate both of the energy efficiency of the power-saving router and the measurement accuracy of Pathload.

A. Simulation settings

Figure 1 depicts the network topology used in the simulation experiments. We assume that a *power-saving router* is connected to a *tight link*, which provides the narrowest bandwidth along the network path between a *sender* and a *receiver*. The maximum physical bandwidth of the tight link is denoted as C_{max}. Other links, labeled as *normal links* in the figure, provide sufficiently wide physical link bandwidth (twice as wide as the tight-link bandwidth). The propagation delay of each link is 5 ms. Cross traffic which traverses the tight link is generated from a *cross traffic sender* to a *cross traffic receiver*. The load of the cross traffic is set to 10% of C_{max}.

With these settings, we use Pathload to measure the available bandwidth between the sender and the receiver. Table I summarizes other parameters of the power-saving router, and the parameters for Pathload are shown in Table II. The total time of each simulation experiment is 100 s. We conduct a Pathload measurement every 10 s, starting at 60 s, and cross traffic is injected from the beginning of the simulation experiments. We set the initial value of the physical link bandwidth of the power-saving router to C_{max}. Therefore, at the beginning of the simulation experiments, the power-saving router gradually decreases its physical

Table II
PARAMETERS OF PATHLOAD

Parameter	Value
Probing packet size	1500 bytes
Number of packets included in a packet stream	25
Number of streams for determining the trend	3
Estimate resolution	1 Mbps
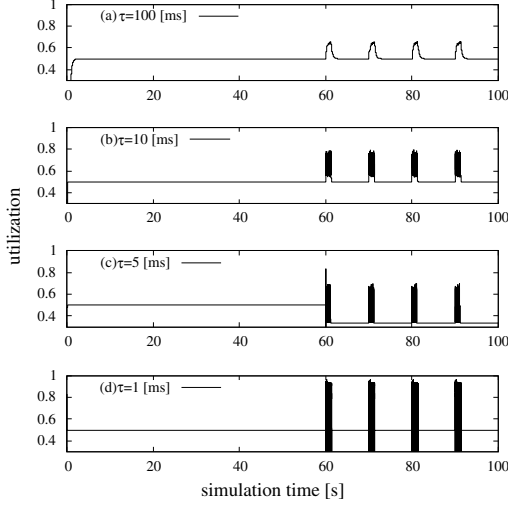
Figure 2. Change in the utilization of the tight link

bandwidth according to the amount of cross traffic.

B. Behavior of the power-saving router

First, we focus on the impact of traffic generated by Pathload during bandwidth probing on the physical bandwidth of the power-saving router. We set C_{max} = 100 Mbps and τ = 100 ms, 10 ms, 5 ms and 1 ms. In Figs. 2 and 3, we plot changes in the average link utilization and the physical link bandwidth, respectively, as functions of the simulation time.

These figures indicate that regardless of the value of τ, the physical link bandwidth and the link utilization converge to 20 Mbps and 0.5, respectively, before Pathload starts the measurement at 60 s. This results from the fact that the power-saving router decreases its physical link bandwidth in order to conserve power. In addition, Fig. 2 shows that the link utilization temporarily increases when Pathload starts measuring the available bandwidth. Specifically, the link utilization increases largely when using small τ. Furthermore, when τ = 5 ms or 1 ms, the power-saving router increases its physical link bandwidth when the measurement starts, as seen in Fig. 3(c)(d). In particular, when τ = 5 ms, the physical link bandwidth increases to 30 Mbps even after the end of the bandwidth measurement. These results clearly demonstrate the adverse effect of bandwidth measurement traffic on the energy efficiency of power-saving routers.
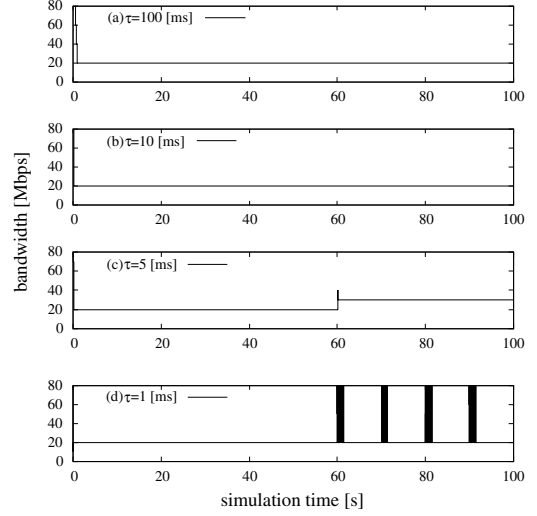
Figure 3. Change in the physical bandwidth of the tight link
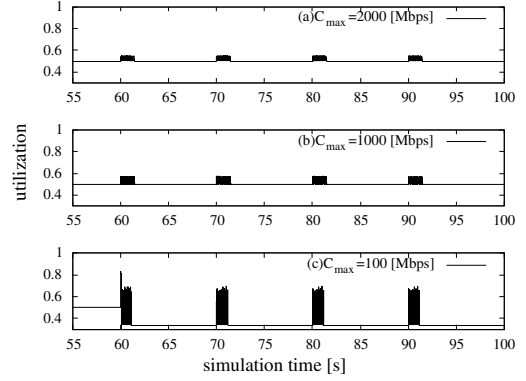
Figure 4. Effect of the maximum bandwidth of the tight link on the utilization

This behavior of the power-saving router is due to the Self-Loading Periodic Streams (SLoPS) algorithm commonly utilized by bandwidth measurement tools, including Pathload. When bandwidth measurement is performed with SLoPS, multiple packets are injected into the network to fill the available/physical bandwidth at the bottleneck link. This procedure increases the utilization of the tight link bandwidth, which in turn causes the power-saving router to increase its physical bandwidth. The differences in the behavior of the router at different values of τ are caused by the algorithm utilized by Pathload, where the sender injects multiple packet streams, each of which consists of multiple packets, into the network at a certain intervals.

Next, we observe the behavior of the power-saving router when τ = 5 ms and the value of C_{max} is varied. In Figs. 4 and 5, we show the changes in link utilization and physical bandwidth of the power-saving router as functions of the simulation time when C_{max} is set to 2000 Mbps, 1000 Mbps and 100 Mbps. We can see from Fig. 4 that
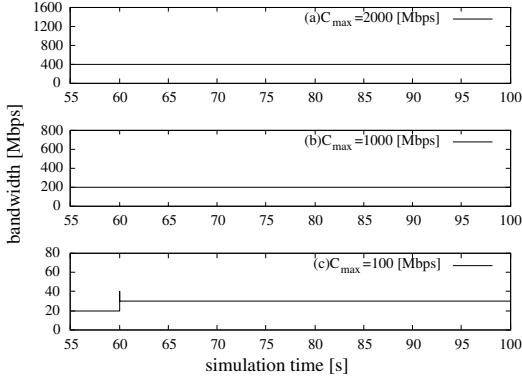
Figure 5. Effect of the maximum bandwidth of the tight link on the physical bandwidth

(a) C_{max} = 2000 Mbps

(b) C_{max} = 1000 Mbps

(c) C_{max} = 100 Mbps

Figure 6. Measurement results obtained with Pathload

the change in link utilization becomes large when C_{max} becomes small. In addition, from Fig. 5, we can observe that although the power-saving router does not increase its physical bandwidth during measurements when C_{max} is 2000 Mbps or 1000 Mbps, it does when C_{max} = 100 Mbps. This behavior of the power-saving router can be explained as follows. First, Pathload sends probing packet streams along the end-to-end network path at a rate that corresponds fairly closely to the true available bandwidth. Second, since each probing packet stream consists of a fixed number of packets regardless of the rate at which streams are dispatched, in order to fill the wider available bandwidth, Pathload sends packet streams at shorter packet intervals, which strongly affects the instantaneous link utilization. Such change in link utilization causes the power-saving router to increase its physical bandwidth, as shown in Fig. 5(c).

C. Measurement accuracy of Pathload

Here, we evaluate the measurement accuracy of Pathload in the presence of a power-saving router. In Fig. 6(a), 6(b), and 6(c), we show the results of measurements conducted with Pathload when C_{max} = 2000 Mbps, 1000 Mbps and 100 Mbps, respectively. We plot the available bandwidth before the measurement together with the Pathload results with error bars since it gives the measurement results as a range of possible values for the available bandwidth.

Figure 6(a) and 6(b) shows that the measurement results obtained with Pathload include the true available bandwidth. This follows from the fact that the physical bandwidth does not change when Pathload starts the measurement, as shown in Fig. 5(a) and 5(b). However, Fig. 6(c) shows that the results obtained with Pathload are far from the true available bandwidth in the case of C_{max} = 100 Mbps since the power-saving router increased its physical link bandwidth due to the measurement load caused by Pathload, as shown in Fig. 5(c). These results indicate that the behavior of the power-saving router degrades the measurement accuracy for the
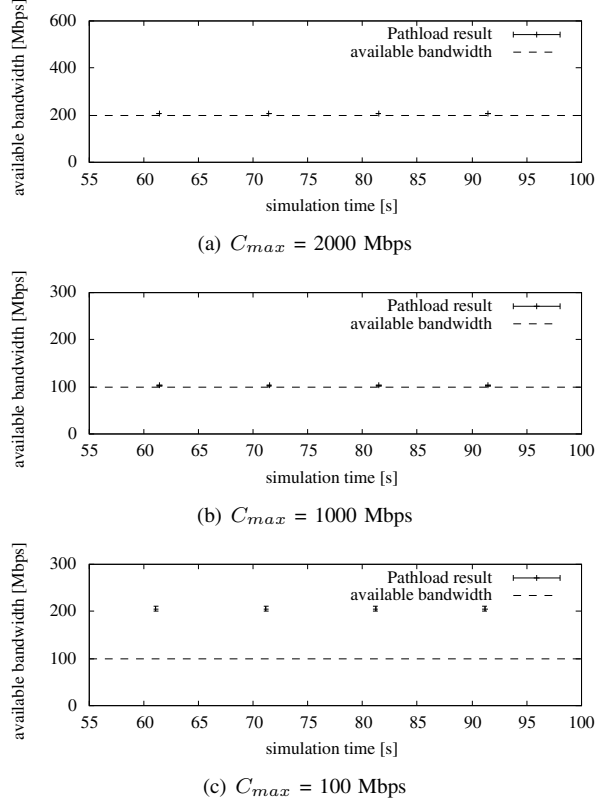
end-to-end available bandwidth.

IV. PARAMETER SETTINGS OF PATHLOAD

In Section III, we indicated that Pathload is unable to measure the available bandwidth accurately when the power-saving router increases its physical bandwidth to accommodate the measurement load caused by Pathload, as well as that changes in the physical bandwidth triggered by the power-saving router degrade its energy efficiency. In this section, we discuss parameter settings for Pathload which ensure that the behavior of the power-saving router remains unaffected. Note that the fundamental ideas in this section can be applied to other measurement tools such as in [5, 6, 11].

A. Pathload algorithm

First, we explain the SLoPS measurement algorithm utilized by Pathload. The sender sends packet streams to the receiver at a certain rate, and as the receiver observes the intervals at which packets in the streams arrive, it compares the intervals with the corresponding sending intervals determined by the sender and estimates the available bandwidth. Finally, the sender adjusts the sending rate of subsequent packet streams according to the observation results provided by the receiver. This cycle is repeated until the algorithm

obtains an estimate of the available bandwidth. The packet streams sent in every cycle are referred to as a *fleet*.

Pathload maintains upper and lower bounds of possible values for the available bandwidth of the end-to-end path and updates these values according to the packet arrival intervals observed by the receiver. We denote the upper bound and the lower bound at the f th cycle as $R_{max}(f)$ and $R_{min}(f)$. In this case, the sender determines $R(f)$, which is the sending rate of a packet stream in the f th cycle, as follows.

$$R(f) = \frac{R_{max}(f) + R_{min}(f)}{2} \qquad (5)$$

The initial value of $R_{min}(0)$ is 0 bps, and $R_{max}(0)$ is determined based on rough estimation of the upper bound of the available bandwidth [14].

When $R(f)$ and the packet size L are given, the sending interval $T(f)$ of packets in packet streams in the fleet of the f th cycle is calculated as follows.

$$T(f) = \frac{L}{R(f)} \qquad (6)$$

The length of the packet stream in the fleet of the f th cycle, denoted as $V_S(f)$, is represented as follows by using Eq. (6) and K, which is the number of packets contained in each packet stream.

$$
\begin{aligned}
V_S(f) &= KT(f) \\
&= \frac{KL}{R(f)} \qquad (7)
\end{aligned}
$$

Note that $V_S(f)$ represents the temporal length of a packet stream in the f th cycle traversing the power-saving router.

B. Pathload parameter settings

Here, we discuss the parameter settings of Pathload which ensure that the behavior of a power-saving router remains unaffected. We assume that the power-saving router has already configured its physical bandwidth according to the current traffic load.

Using Eqs. (3) and (4), the conditions for the power-saving router to maintain its physical bandwidth are as follows.

$$
\begin{aligned}
U(t) &= (1-w)U(t-1) + wu(t) \\
&= w\sum_{k=1}^{t}(1-w)^{t-k}u(k) \\
&\leq \lambda_u \qquad (8)
\end{aligned}
$$

We divide $P(t)$, which is the amount of traffic observed at the tight link, into $P^L(t)$ and $P^C(t)$ as follows.

$$P(t) = P^L(t) + P^C(t) \qquad (9)$$

where $P^L(t)$ indicates the amount of traffic caused by Pathload while measuring the available bandwidth which arrives at the tight link at the t th time slot, and $P^C(t)$ is
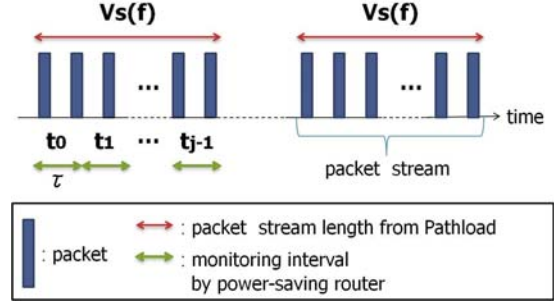
Figure 7. Relationship between packet stream length and monitoring interval

the amount of cross traffic. By using Eqs. (2), (3) and (9), the average link utilization $U(t)$ can be rewritten as follows.

$$
\begin{aligned}
U(t) &= w\sum_{k=1}^{t}(1-w)^{t-k}u(k) \\
&= w\sum_{k=1}^{t}(1-w)^{t-k}\frac{P^L(k) + P^C(k)}{C(t)\tau} \\
&= w\sum_{k=1}^{t}(1-w)^{t-k}\frac{P^L(k)}{C(t)\tau} + \\
&\quad w\sum_{k=1}^{t}(1-w)^{t-k}\frac{P^C(k)}{C(t)\tau} \qquad (10)
\end{aligned}
$$

The first term in Eq. (10) represents traffic contributed by Pathload while measuring the link utilization, and the second term represents cross traffic. Assuming cross traffic arriving at the tight link at a fixed rate R^C, Eq. (10) can be rewritten as follows.

$$U(t) = w\sum_{k=1}^{t}(1-w)^{t-k}\frac{P^L(k)}{C(t)\tau} + \frac{R^C}{C(t)} \qquad (11)$$

In the following discussion, we assume $\tau \leq V_S(f)$, in other words, a utilization monitoring interval is shorter than the length of the packet stream sent by Pathload since in such cases the measurement traffic generated by Pathload strongly influences the behavior of power-saving routers. For simplicity, we assume $V_S(f) = j\tau$, where j is an integer greater than one. The relationship between packet stream length and monitoring interval is presented in Fig. 7, where the power-saving router monitors the probing packet stream for time slots $t_0, t_1, \ldots, t_{j-1}$. Since the arrival rate of packet steams corresponds closely to the available bandwidth, the link utilization increases considerably, particularly when the packet stream spans multiple monitoring intervals of link utilization, which are denoted as time slots $t_0, \ldots, t_{j-1}$ in Fig. 7. In this situation, Eq. (8) can be rewritten based on Eq. (11), assuming that the interval between two packet streams is sufficiently large not to affect the calculation of average

link utilization in Eq. (3).

$$U(t_{j-1}) = w \sum_{k=0}^{j-1} (1-w)^{j-1-k} \frac{R(f)}{C(t)} + \frac{R^C}{C(t)}$$
$$\leq \lambda_u \qquad (12)$$

Note that we can control only j to satisfy Eq. (12), which is achieved by changing K (the number of packets contained in the packet stream). Therefore, by configuring the number of packets in each packer stream to satisfy Eq. (12), we can prevent Pathload from affecting the behavior of power-saving routers.

C. Verification

We verify the validity of Eq. (12) through comparison with the simulation results in Figs. 2 and 3. Specifically, we utilize Figs. 2(b)(c)(d) and 3(b)(c)(d) to assess Eq. (12) because of the constraint of $\tau \leq V_S(f)$. We assume the highest rate of packet streams in the simulation, which is 16 Mbps. In this case, $U(t)$ in Eq. (12) becomes 0.74, 0.88 and 1.07 when τ is 10 ms, 5 ms and 1 ms, respectively. Since λ_u is 0.8, we expect an increase in the physical bandwidth when τ is set to 5 ms or 1 ms. Figure 3 confirms the expectation that the physical bandwidth remains unchanged only for $\tau = 10$ ms (Fig. 3(b)) while the physical bandwidth increases when the measurement is started (Fig. 3(c) and (d) with $\tau = 5$ ms and 1 ms, respectively). The above results confirm the validity of Eq. (12) in terms of providing the conditions where the energy efficiency of power-saving routers remains unaffected.

V. CONCLUSION

In this paper, we evaluated the performance of Pathload in a network environment with a power-saving router. Through extensive simulation results, we confirmed that accurate measurement results are difficult to obtain, particularly when the interval for monitoring the link utilization of the power-saving router is short and the physical bandwidth of the tight link is narrow. We also obtained the parameter settings of Pathload for which the behavior of the power-saving router remains unaffected.

In future work, we plan to enhance the algorithm of Pathload to accommodate power-saving routers by implementing automatic parameter setting to avoid the adverse effects of traffic generated by Pathload on the energy efficiency of power-saving routers. We also plan to evaluate the performance of Pathload in a network environment with power-saving routers and the energy efficiency of power-saving routers more detailed.

ACKNOWLEDGMENT

REFERENCES

[1] R. Kubo, J. Kani, H. Ujikawa, Y. Fujimoto, N. Yoshimoto, and H. Hadama, "Study and demonstration of sleep and adaptive link rate control mechanisms for energy efficient 10G-EPON," *IEEE/OSA Journal of Optical Communications and Networking*, vol. 2, no. 9, pp. 716 –729, September 2010.

[2] F. Blanquicet and K. Christensen, "An initial performance evaluation of rapid PHY selection (RPS) for energy efficient ethernet," in *Proceedings of the 32nd IEEE Conference on Local Computer Networks*, pp. 223–225, October 2007.

[3] G. Ginis, "Low-power modes for ADSL2 and ADSL2+," White paper, Broadband Communications Group, Texas Instruments, January 2005.

[4] M. Jain and C. Dovrolis, "End-to-end available bandwidth: Measurement methodology, dynamics, and relation with TCP throughput," in *Proceedings of ACM SIGCOMM 2002*, pp. 295–308, July 2002.

[5] C. L. T. Man, G. Hasegawa, and M. Murata, "ImTCP: TCP with an inline measurement mechanism for available bandwidth," in *Computer Communications Journal special issue of Monitoring and Measurements of IP Networks*, pp. 1614–1626, June 2006.

[6] V. J. Ribeiro, R. H. Riedi, R. G. Baraniuk, J. Navratil, and L. Cottrell, "pathChirp: Efficient available bandwidth estimation for network paths," in *Proceedings of Passive and Active Measurements (PAM) Workshop*, pp. 1–11, April 2003.

[7] J. Strauss, D. Katabi, and F. Kaashoek, "A measurement study of available bandwidth estimation tools," in *Proceedings of the 3rd ACM SIGCOMM conference on Internet measurement*, pp. 39–44, October 2003.

[8] R. L. Carter and M. E. Crovella, "Measuring bottleneck link speed in packet-switched networks," *Performance Evaluation*, pp. 297–318, March 1996.

[9] A. Downey, "Using pathchar to estimate Internet link characteristics," in *Proceedings of ACM SIGCOMM'99*, pp. 241–250, October 1999.

[10] Pchar, available at http://www.kitchenlab.org/www/bmah/Software/pchar/.

[11] N. Hu and P. Steenkiste, "Evaluation and characterization of available bandwidth probing techniques," *IEEE Journal on Selected Areas in Communications*, vol. 21, no. 6, pp. 879 –894, August 2003.

[12] S. Ata, K. Yonezaki, and I. Oka, "A method of traffic prediction for performance adjustable energy-aware routers," *IEICE technical report*, vol. 111, no. 43, pp. 121–126, May 2011, (in Japanese).

[13] The VINT Project, "UCB/LBNL/VINT network simulator - ns (version 2)."

[14] M. Jain and C. Dovrolis, "Pathload: A measurement tool for End-to-End available bandwidth," in *Proceedings of Passive and Active Measurements (PAM) Workshop*, pp. 14–25, March 2002.